Lattice Effects Observed in Chaotic Dynamics of Experimental Populations

Shandelle M. Henson,[1]* R. F. Costantino,[2] J. M. Cushing,[3] Robert A. Desharnais,[4] Brian Dennis,[5] Aaron A. King[6]

Animals and many plants are counted in discrete units. The collection of possible values (state space) of population numbers is thus a nonnegative integer lattice. Despite this fact, many mathematical population models assume a continuum of system states. The complex dynamics, such as chaos, often displayed by such continuous-state models have stimulated much ecological research; yet discrete-state models with bounded population size can display only cyclic behavior. Motivated by data from a population experiment, we compared the predictions of discrete-state and continuous-state population models. Neither the discrete- nor continuous-state models completely account for the data. Rather, the observed dynamics are explained by a stochastic blending of the chaotic dynamics predicted by the continuous-state model and the cyclic dynamics predicted by the discrete-state models. We suggest that such lattice effects could be an important component of natural population fluctuations.

The discovery that simple deterministic population models can display complex aperiodic fluctuations such as chaos (*1*) inspired decades of empirical and theoretical work in ecology (*2*, *3*). Such mathematical models of population dynamics make use of a continuous state space, i.e., variables representing population densities are real-valued. But animals, and for many practical purposes, plants, come in whole numbers. More realistic models would cast population densities as discrete variables, with state space a discrete lattice of numbers. As long as population size is bounded, deterministic models of the latter type have finitely many possible states and hence display only periodic cycles. Approximating population size with continuous-state models is commonly justified by the assumption that population numbers remain sufficiently large so that the discrete state space lattice is sufficiently fine (*4*). However, the deterministic dynamics of associated discrete-state and continuous-state models can be quite different even for very large population sizes, so that the "lattice effects" caused by the discreteness of animal densities cannot always be ignored (*5*).

Of course, real ecological systems are invariably stochastic. The relative degree of stochastic variability due to random demographic events experienced by individuals (births, deaths) is known to increase at low population numbers. The increased variability is just the law of large numbers in reverse: If, out of a population of 10,000, individuals each die at random with probability $(1 - p)$, the number of survivors is (relatively) near the expected value of $10{,}000p$, whereas if the initial population were only 10 individuals, the relative departure of survivors from $10p$ is likely to be more extreme. The increased variability of populations under demographic noise at small population sizes is a well-studied theme of discrete-state population models (*4*, *6*). Here we show how the deterministic component of dynamics on the discrete lattice of population values can influence stochastic population dynamics at both high and low population sizes, over and above the influence of demographic stochastic forces. Intriguingly, the pattern of the stochastic dynamics emerges as a blend of the patterns predicted by the continuous- and discrete-state models. Moreover, we report on a laboratory population experiment that demonstrates that such lattice effects are in fact both real and important.

We illustrate population lattice effects with the Ricker map (*7*, *8*), a simple model familiar in ecology and chaos theory (*1*, *9*). The model

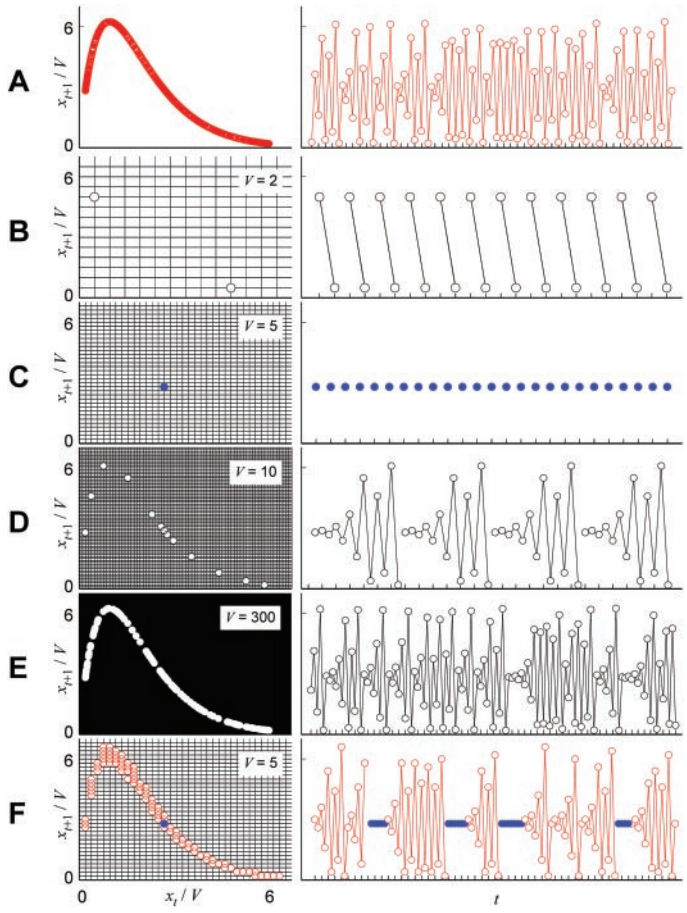

Fig. 1. Density dynamics of Ricker models with $b = 17$ and $c = 1$. Phase plots are shown on the left, and the corresponding time series on the right. (**A**) The chaotic attractor of Ricker model Eq. 1. (**B**) A 2-cycle attractor of the lattice Ricker model Eq. 2 with $V = 2$ (196 displayed lattice points). (**C**) Equilibrium attractor of lattice model Eq. 2 with $V = 5$ (1225 displayed lattice points). (**D**) A 13-cycle attractor of lattice model Eq. 2 with $V = 10$ (4900 displayed lattice points), which begins to resemble the chaotic attractor in (A). (**E**) A 117-cycle attractor of lattice model Eq. 2 with $V = 300$ (4.41×10^6 displayed lattice points), which highly resembles the chaotic attractor in (A). Notice that the lattice is so fine with $V = 300$ that the grid lines appear to fill the entire space. (**F**) A stochastic realization of the stochastic lattice model Eq. 3 with $V = 5$ and $\sigma = 0.03$. Noise on the lattice reveals the chaotic signal, but episodes (colored in blue) of the lattice equilibrium in (C) recur.

[1]Department of Mathematics, Andrews University, Berrien Springs, MI 49104, USA. [2]Department of Biological Sciences, University of Rhode Island, Kingston, RI 02881, USA. [3]Department of Mathematics, Interdisciplinary Program in Applied Mathematics, University of Arizona, Tucson, AZ 85721, USA. [4]Department of Biology and Microbiology, California State University, Los Angeles, CA 90032, USA. [5]Department of Fish and Wildlife Resources and Division of Statistics, University of Idaho, Moscow, ID 83844, USA. [6]Department of Environmental Science and Policy, University of California, Davis, CA 95616, USA.

*To whom correspondence should be addressed. E-mail: henson@andrews.edu

takes the form $y_{t+1} = by_t \exp(-cy_t)$, where y_t represents the density of individuals per unit habitat size at time t, $b > 0$ is the per capita birth rate, and $\exp(-cy_t)$ (with $c > 0$) is the fraction of offspring expected to survive one unit of time at population density y_t. The exponential term that occurs here and in the sequel can be interpreted as arising from an assumption of random contacts among individuals. Examples of such processes include contacts among hosts and parasitoids (*10*–*12*), and the cannibalistic interactions in *Tribolium* (*13*, *14*) and *Plodia* (*15*). It is well known that the Ricker and similar models can exhibit complex dynamics, including chaos.

We introduce habitat size V explicitly into the model equation by the change of variables $x_t = y_t V$, where x_t is the number of individuals in a habitat of size V. For the Ricker map this leads to the equation

$$x_{t+1} = bx_t \exp\left(-\frac{c}{V}x_t\right) \quad (1)$$

The density-dependence coefficient $\frac{c}{V}$ is now inversely proportional to the habitat size. In this type of model, density dynamics are invariant with respect to V (i.e., the sequence $\{x_t\}_{t=0}^{\infty}$ is a solution of Eq. 1 when $V = 1$ if and only if the sequence $\{kx_t\}_{t=0}^{\infty}$ is a solution when $V = k$). For example, a population displaying a 2-cycle oscillation in a 2-acre habitat is forecast also to display 2-cycles in a 200-acre habitat, with a 100-fold increase in animal numbers. Empirical studies show that some species scale with habitat size in this fashion (*16*); however, this scaling law breaks down in unrealistically small (or large) habitat sizes. Here we focus on the class of models whose continuous-state dynamics scale with habitat size V, and vary the parameter V to compare populations of various sizes in corresponding discrete-state models.

Suppose we confine the model in Eq. 1 to the lattice of feasible states by means of the integerization

$$x_{t+1} = \mathrm{int}\left[bx_t \exp\left(-\frac{c}{V}x_t\right)\right] \quad (2)$$

where int[x] denotes the nearest integer to x (0.5's are rounded up). For parameter values at which Eq. 1 is chaotic (Fig. 1A), the dynamics of the "lattice model" in Eq. 2 range through a complicated sequence of transitions, including a 2-cycle when $V = 2$ (Fig. 1B), an equilibrium when $V = 5$ (Fig. 1C), a 13-cycle when $V = 10$ (Fig. 1D), and a 117-cycle resembling the chaotic attractor when $V = 300$ (Fig. 1E). In terms of density, as V increases (i.e., as the density lattice spacing decreases), the attractors of the lattice model eventually resemble the chaotic attractor of Eq. 1. However, this increase in complexity is not monotone. Each of the attractors in Fig. 1, B to E, is an approximation of the chaotic attractor in Fig. 1A, although the underlying complexity of the continuum limit cannot be observed deterministically unless the habitat is of sufficiently large size (i.e., the density lattice is sufficiently fine).

Even on a coarse density lattice, the underlying deterministic complexity can be revealed by noise as the system is stirred into continual transient behavior. For example, a stochastic version of Eq. 2 is

$$x_{t+1} = \mathrm{int}\left[bx_t \exp\left(-\frac{c}{V}x_t + \sigma z_t\right)\right] \quad (3)$$

where z_t is a standard normal random variable and σ measures the intensity of the noise. When $V = 5$, the deterministic lattice model in Eq. 2 predicts an equilibrium (Fig. 1C); however, typical orbits of the stochastic lattice model in Eq. 3 reveal features similar to those of the chaotic attractor (Fig. 1F). Note that the stochastic time series in Fig. 1F episodically revisits the equilibrium of the deterministic lattice model (Fig. 1C).

The integerized Ricker model (Eq. 2) illustrates what we call a "lattice effect," i.e., a significant effect of discrete state space granularity on the dynamics of a population. As seen in Fig. 1, lattice effects can occur in both deterministic systems (Figs. 1, B to E) and stochastic systems (Fig. 1F). In deterministic systems, the complexity of underlying chaotic dynamics obscured by lattice effects is revealed by sufficiently refining the lattice (e.g., by increasing the habitat volume). However, even for coarse lattices, features of the complexity might be revealed by the presence of noise on the lattice. In this latter case, the system typically retains episodic reappearances of the lattice dynamic.

Lattice effects in models are quite general. Figure 2 shows lattice effects in a parasitoid-host model (*17*). In Fig. 2E the stochastic lattice model time series episodically resembles both the deterministic chaotic attractor (Fig. 2A) and the deterministic lattice model 4-cycle (Fig. 2C).

Lattice effects are not theoretical oddities arising from simple population models. We report here observations of lattice effects in an experimental study. This example comes from a study involving the flour beetle *Tribolium* (*3*,

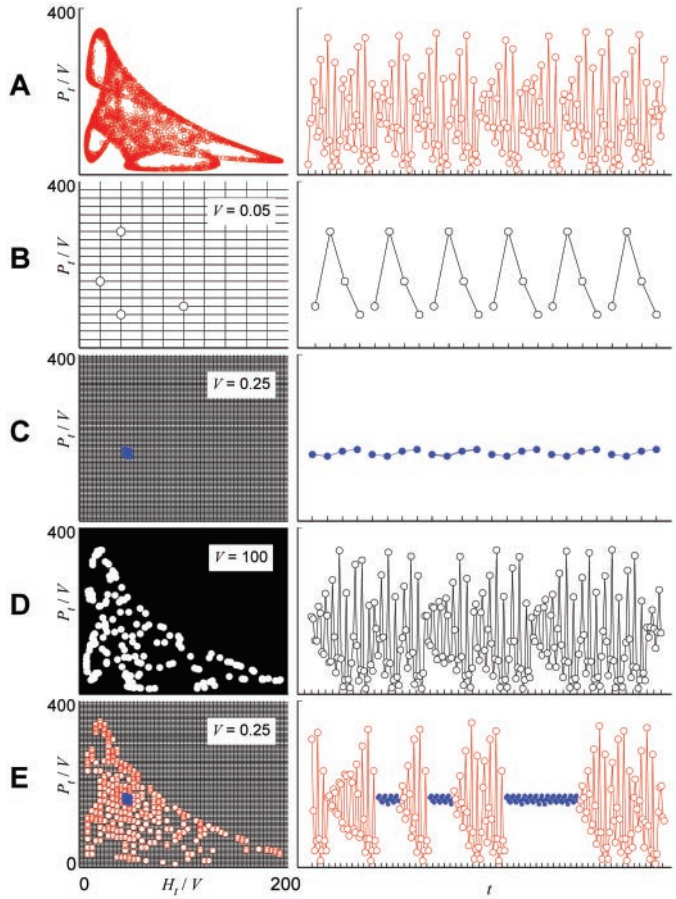

Fig. 2. Density dynamics of a modified Nicholson-Bailey parasitoid-host model (*17*) in which the area of discovery is inversely proportional to the habitat size V. The lattice model equations are $H_{t+1} = \mathrm{int}(H_t \exp[r(1 - H_t/(KV)) - aP_t/V])$ and $P_{t+1} = \mathrm{int}(sH_t[1 - \exp(-aP_t/V)])$. We used parameter values $r = 3$, $K = 100$, $a = 0.01$, $s = 4.4$ and initial conditions $H_0 = 100V$, $P_0 = 100V$. (**A**) The chaotic attractor of the nonlattice model. (**B**) A high-amplitude 4-cycle attractor of the lattice model with $V = 0.05$ (200 displayed lattice points). (**C**) A low-amplitude 4-cycle attractor of the lattice model with $V = 0.25$ (5000 displayed lattice points). (**D**) A 181-cycle attractor of the lattice model with $V = 100$ (8×10^8 displayed grid points), which resembles the chaotic attractor in (A). (**E**) A stochastic realization of the parasitoid-host model with noise added on the square-root scale before integerization [appropriate for demographic noise (*3*)]. The equations are $H_{t+1} = \mathrm{int}([\sqrt{H_t}\exp[r(1 - H_t/(KV)) - aP_t/V] + \sigma_1 z_{1t}]^2)$ and $P_{t+1} = \mathrm{int}([\sqrt{sH_t[1 - \exp(-aP_t/V)]} + \sigma_2 z_{2t}]^2)$. Here z_{1t} and z_{2t} are standard normal random variables and σ_i measures the intensity of the noise. In these simulations we used $\sigma_1 = \sigma_2 = 0.01$. The stochastic orbit exhibits a mixture of patterns, occasionally resembling the low-amplitude 4-cycle attractor of the lattice model in (C) (colored in blue), and occasionally resembling the time series of the chaotic attractor of the nonlattice model in (A) (colored in red).

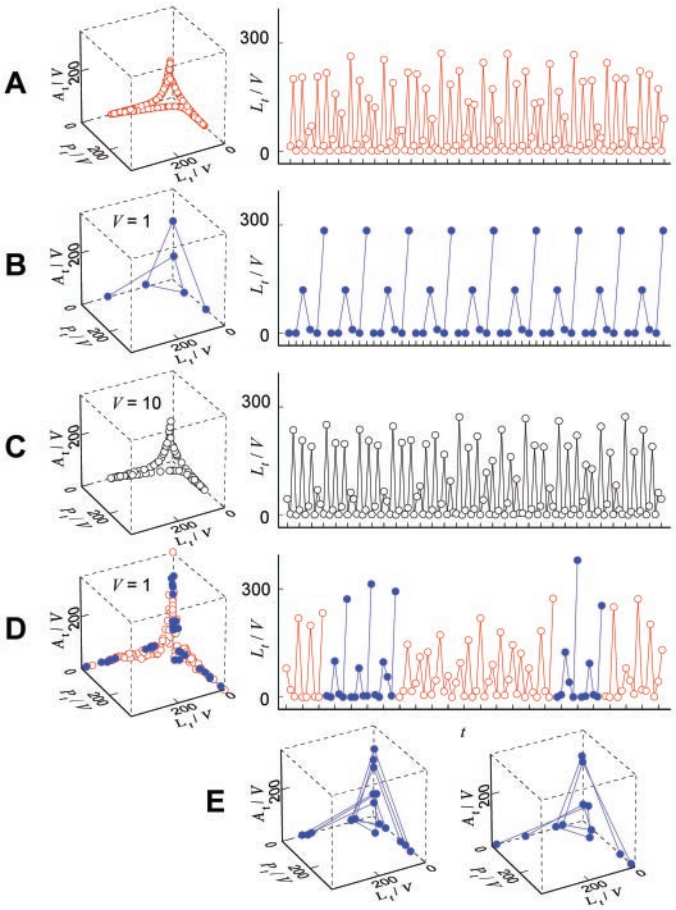

Fig. 3. Density dynamics of the LPA models with b = 10.67, μ_l = 0.1955, μ_a = 0.96, c_{el} = 0.01647, c_{ea} = 0.01313, c_{pa} = 0.35. For the stochastic model (*32*), the variance and covariance entries of the matrix Σ were taken to be σ_{11} = 2.332, σ_{22} = 0.2374, and σ_{12} = σ_{21} = 0 (*3*). (**A**) The chaotic attractor of LPA model (*19*). (**B**) A 6-cycle attractor of the lattice LPA model (*31*) with V = 1 (on the order of 10^7 lattice points). (**C**) A 124-cycle attractor of lattice model (*31*) with V = 10 (on the order of 10^{10} lattice points), which resembles the chaotic attractor in (A). (**D**) A stochastic realization of (*32*) with V = 1 exhibits a mixture of patterns, with intermittent patterns (colored in blue) that resemble the lattice 6-cycle in (B) interspersed among episodes (colored in red) that resemble the chaotic attractor in (A). (**E**) The 6-patterns in (D) are shown in phase space, where their resemblance to the 6-cycle in (B) is apparent.

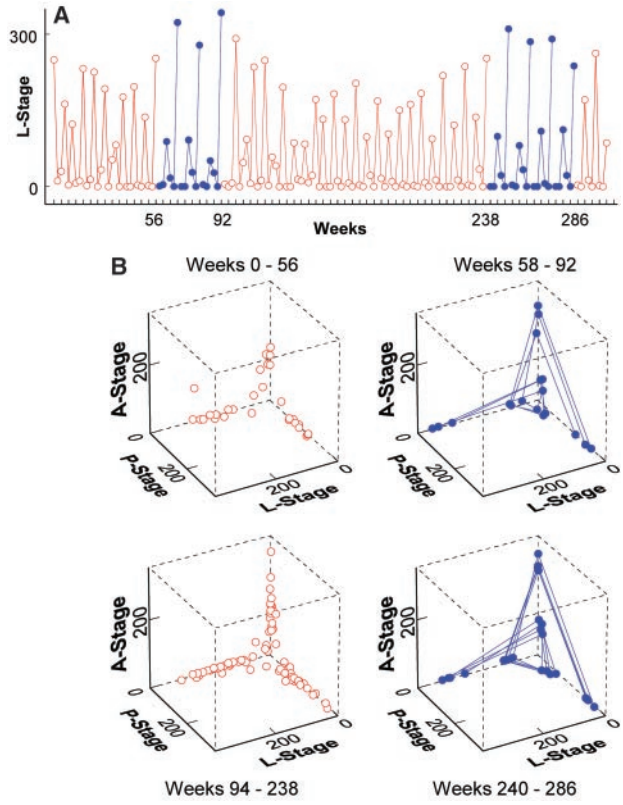

Fig. 4. A 304-week data time series obtained from one replicate of the *Tribolium* experiment (*3*). Parameter values (*3*) for the experiment are b = 10.67, μ_l = 0.1955, μ_a = 0.96, c_{el} = 0.01647, c_{ea} = 0.01313, and c_{pa} = 0.35. (**A**) Selected temporal episodes that resemble the lattice model 6-cycle shown in Fig. 3B are colored in blue. The remaining data points, colored in red, resemble the chaotic time series. (**B**) The selected temporal episodes in (A) are shown in phase space (on the order of 10^7 lattice points). Compare the blue 6-pattern episodes to the 6-cycle lattice attractor in Fig. 3B.

18) whose chaotic cultures we have maintained for over 6 years. The experimental design was based on the predictions of the deterministic "LPA model" (*19*). The LPA model has successfully explained and predicted nonlinear phenomena in a variety of contexts, including transitions between dynamic regimes, multiple attractors, resonance, phase switching, and saddle influences (*3*, *18*, *20*–*30*). As in the Ricker model, the density dynamics of the LPA model are invariant with respect to habitat size V, and the continuous state variables L_t, P_t, and A_t are not confined to the lattice of feasible states.

The LPA model predicts sequences of dynamic bifurcations as parameters are varied, including bifurcation routes to chaos. One such sequence was used to design the laboratory experiment mentioned above. In this experiment the forecast route to chaos was experimentally induced by manipulating the adult death rate and adult recruitment rate (*3*, *18*, *24*). Experimental treatments were placed in seven different predicted dynamic regimes across the bifurcation sequence. In each treatment, including those forecast to be chaotic, the data display the predicted dynamics (*3*, *24*). However, a close study of the data also reveals seemingly anomalous patterns not predicted by the LPA model—patterns that are, however, predicted by lattice versions of the LPA model. We present one example in detail. Figure 3A shows a chaotic attractor of the LPA model from the predicted bifurcation sequence. The data from the experimental treatment corresponding to this attractor exhibit the temporal and phase space patterns of the predicted chaotic dynamics (*3*, *24*). However, the data also reveal a near 6-cycle pattern not predicted by the LPA model. We show that this unexpected 6-pattern is in fact a lattice effect.

We integerized the LPA model to simulate lattice dynamics (*31*). When V = 1, the lattice model predicts a 6-cycle attractor (Fig. 3B). When V = 10, the lattice model predicts a 124-cycle (Fig. 3C) resembling the chaotic attractor (Fig. 3A). As V increases, the lattice attractors range through a complicated sequence of transitions, but eventually converge on the chaotic attractor of the LPA model.

The lattice 6-cycle in Fig. 3B (predicted when V = 1, the habitat size used in the experimental study) closely resembles the 6-pattern appearing episodically in the data (see Fig. 4). Although the integerization of the LPA model given in (*31*) is somewhat arbitrary, other integerizations yielded the same result.

A stochastic version (*32*) of the integerized LPA model is obtained by adding demographic noise on the square-root scale to the two unmanipulated life-stage equations, namely the larval and pupal equations (*3*). When V = 1, the time series generated by the stochastic lattice model resembles the chaotic

attractor; however, the lattice effect 6-pattern episodically recurs (see Fig. 3, D and E).

The 6-pattern forecast by the stochastic lattice model is evident in the three experimental replicates (*3*, *18*). Figure 4A shows the larval time series data from one replicate. The intermittently occurring 6-pattern is also seen in the phase space representation of the data (Fig. 4B).

Lattice effects can dramatically alter the predictions of ecological models, especially in systems for which the continuous-state deterministic dynamics are complex. In deterministic models, discretizing state space can replace a complicated continuous-state attractor with a simpler lattice attractor; yet the continuous-state dynamics remain important, inasmuch as they continue to shape the transient behavior on the lattice. In the presence of noise, the system is influenced by both transients and attractors, and thus displays episodes that alternately resemble the dynamics of the continuous-state and lattice models. We emphasize that such lattice effects are not only found in relatively coarse lattices or in small populations; indeed, in our experimental study of chaotic population dynamics, lattice effects were important even with 10^7 lattice points.

A primary goal of ecology is the understanding of population fluctuations. Our evidence demonstrates that the traditional focus on continuous-state models is too narrow. Specifically, important effects in population dynamics due to the discrete nature of organisms may be entirely missed by continuous-state models, yet follow as straightforward predictions of lattice models. We suggest that a complete understanding of some population systems will require a blend of both continuous-state and discrete-state models.

References and Notes

1. R. M. May, *Science* **186**, 645 (1974).
2. A. Hastings, C. L. Hom, S. Ellner, P. Turchin, H. C. J. Godfray, *Annu. Rev. Ecol. Syst.* **24**, (1993).
3. B. Dennis, R. A. Desharnais, J. M. Cushing, S. M. Henson, R. F. Costantino, *Ecol. Monogr.* **71**, 277 (2001).
4. R. M. May, *Stability and Complexity in Model Ecosystems* (Princeton Univ. Press, Princeton, NJ, ed. 2, 1974).
5. E. A. Jackson, *Perspectives of Nonlinear Dynamics* (Cambridge Univ. Press, Cambridge, 1989), vol. 1, pp. 216–219.
6. H. B. Wilson, M. P. Hassell, *Proc. R. Soc. London B* **264**, 1189 (1997).
7. P. A. P. Moran, *Biometrics* **6**, 250 (1950).
8. W. E. Ricker, *J. Fish. Res. Board Can.* **11**, 559 (1954).
9. R. M. May, G. F. Oster, *Am. Nat.* **110**, 573 (1976).
10. A. J. Nicholson, *J. Anim. Ecol.* **2**, 132 (1933).
11. _____, V. A. Bailey, *Proc. Zool. Soc. London*, 551 (1935).
12. M. P. Hassell, *J. Anim. Ecol.* **69**, 543 (2000).
13. A. C. Crombie, *Proc. R. Soc. London B.* **133**, 76 (1946).
14. R. F. Costantino, R. A. Desharnais, *Population Dynamics and the* Tribolium *Model: Genetics and Demography* (Springer, New York, 1991).
15. C. J. Briggs, S. M. Sait, M. Begon, D. J. Thompson, H. C. J. Godfray, *J. Anim. Ecol.* **69**, 352 (2000).
16. R. N. Chapman, *Ecology* **9**, 111 (1928).
17. J. R. Beddington, C. A. Free, J. H. Lawton, *Nature* **255**, 58 (1975).
18. R. F. Costantino, R. A. Desharnais, J. M. Cushing, B. Dennis, *Science* **275**, 389 (1997).
19. The LPA model is

$$L_{t+1} = bA_t \exp\left(-\frac{c_{ea}}{V}A_t - \frac{c_{el}}{V}L_t\right),$$

$$P_{t+1} = (1-\mu_l)L_t,$$

$$A_{t+1} = P_t \exp\left(-\frac{c_{pa}}{V}A_t\right) + (1-\mu_a)A_t.$$

Here L_t, P_t, and A_t are, respectively, the number of feeding larvae at time t; the number of nonfeeding larvae, pupae, and callow adults at time t; and the number of sexually mature adults at time t. The unit of time is 2 weeks, which is the approximate amount of time spent in each of the L and P classes under experimental conditions. $b > 0$ is the average number of larvae recruited per adult per unit time in the absence of cannibalism, and the fractions μ_a and μ_l are the adult and larval probabilities of dying from causes other than cannibalism in one time unit. The exponentials represent the fractions of individuals surviving cannibalism one unit of time, with "cannibalism coefficients" c_{ea}/V, c_{el}/V, $c_{pa}/V > 0$. Habitat size V has units equal to the volume occupied by 20 g of flour, the amount of medium routinely used in our laboratory.
20. R. F. Costantino, J. M. Cushing, B. Dennis, R. A. Desharnais, S. M. Henson, *Bull. Math. Biol.* **60**, 247 (1998).
21. R. F. Costantino, J. M. Cushing, B. Dennis, R. A. Desharnais, *Nature* **375**, 227 (1995).
22. J. M. Cushing, B. Dennis, R. A. Desharnais, R. F. Costantino, *Ecol. Model.* **92**, 111 (1996).
23. _____, *J. Anim. Ecol.* **67**, 298 (1998).
24. J. M. Cushing *et al.*, *Chaos Solitons Fractals* **12**, 219 (2001).
25. B. Dennis, R. A. Desharnais, J. M. Cushing, R. F. Costantino, *Ecol. Monogr.* **65**, 261 (1995).
26. _____, *J. Anim. Ecol.* **66**, 704 (1997).
27. R. A. Desharnais, R. F. Costantino, J. M. Cushing, B. Dennis, *Science* **276**, 1881 (1997).
28. R. A. Desharnais, R. F. Costantino, J. M. Cushing, S. M. Henson, B. Dennis, *Ecol. Lett.* **4**, 229 (2001).
29. S. M. Henson, J. M. Cushing, R. F. Costantino, B. Dennis, R. A. Desharnais, *Proc. R. Soc. London B* **265**, 2229 (1998).
30. S. M. Henson, R. F. Costantino, J. M. Cushing, B. Dennis, R. A. Desharnais, *Bull. Math. Biol.* **61**, 1121 (1999).
31. In the experimental protocol, the parameters μ_a and c_{pa} were manipulated by means of the necessarily integerized equation

$$A_{t+1} = \mathrm{int}\left[P_t \exp\left(-\frac{c_{pa}}{V}A_t\right)\right] + \mathrm{int}[(1-\mu_a)A_t].$$

Thus, one possible deterministic lattice model for the experiment in question, and the one used here, is

$$L_{t+1} = \mathrm{int}\left[bA_t \exp\left(-\frac{c_{ea}}{V}A_t - \frac{c_{el}}{V}L_t\right)\right],$$

$$P_{t+1} = \mathrm{int}[(1-\mu_l)L_t],$$

$$A_{t+1} = \mathrm{int}\left[P_t \exp\left(-\frac{c_{pa}}{V}A_t\right)\right] + \mathrm{int}[(1-\mu_a)A_t].$$

32. The stochastic lattice model used here is

$$L_{t+1} = \mathrm{int}\left[\left(\sqrt{bA_t \exp\left(-\frac{c_{ea}}{V}A_t - \frac{c_{el}}{V}L_t\right)} + E_{1t}\right)^2\right],$$

$$P_{t+1} = \mathrm{int}[(\sqrt{(1-\mu_l)L_t} + E_{2t})^2],$$

$$A_{t+1} = \mathrm{int}\left[P_t \exp\left(-\frac{c_{pa}}{V}A_t\right)\right] + \mathrm{int}[(1-\mu_a)A_t].$$

where E_{1t} and E_{2t} are random normal variables with mean zero and variance-covariance matrix Σ. In the rare cases in which a large negative E causes a negative value inside a square, we set the right-hand side of that equation equal to zero.

33. We thank E. W. Davis, J. Delos, and W. M. Schaffer for comments. Supported in part by the National Science Foundation (grants DMS 9973126, 9981374, 9981423, 9981458), a Howard Hughes Medical Institute grant to the College of William and Mary (S.M.H.), and an NSF Mathematical Sciences Postdoctoral Research Fellowship (A.A.K.).

12 June 2001; accepted 29 August 2001

Regulation of Cutaneous Malignancy by γδ T Cells

Michael Girardi,[1]* David E. Oppenheim,[2]* Carrie R. Steele,[2] Julia M. Lewis,[1] Earl Glusac,[1] Renata Filler,[1] Paul Hobby,[3] Brian Sutton,[3] Robert E. Tigelaar,[1] Adrian C. Hayday[2]†

The localization of γδ T cells within epithelia suggests that these cells may contribute to the down-regulation of epithelial malignancies. We report that mice lacking γδ cells are highly susceptible to multiple regimens of cutaneous carcinogenesis. After exposure to carcinogens, skin cells expressed Rae-1 and H60, major histocompatibility complex–related molecules structurally resembling human MICA. Each of these is a ligand for NKG2d, a receptor expressed by cytolytic T cells and natural killer (NK) cells. In vitro, skin-associated NKG2d$^+$ γδ cells killed skin carcinoma cells by a mechanism that was sensitive to blocking NKG2d engagement. Thus, local T cells may use evolutionarily conserved proteins to negatively regulate malignancy.

A substantial fraction of the T cell pool is constitutively resident within epithelia. These intraepithelial lymphocytes (IELs) display limited T cell receptor (TCR) diversity and may recognize autologous proteins expressed on epithelial cells after infection or malignant transformation (*1*). Consistent with this, human bowel carcinomas show up-regulated expression of two major histocompatibility complex (MHC) class I–related molecules, MICA and MICB, and are targets for cytolysis by intestinal TCRγδ$^+$ IELs expressing NKG2d, a receptor for MICA and MICB (*2*). Nonetheless, the capacity of either γδ cells or MICA to regulate malignancy in vivo is